Journal of Alloys and Compounds 509S (2011) S684–S687

Contents lists available at ScienceDirect

Journal of Alloys and Compounds

journal homepage: www.elsevier.com/locate/jallcom

Mechano-chemical reactions in $\text{LiBH}_4 + \text{VCl}_n$ ($n = 2$ and 3) mixtures

Isabel Llamas-Jansa*, Nadir Aliouane, Stefano Deledda, Jon Erling Fonneløp, Christoph Frommen, Klaus Lieutenant, Sabrina Sartori, Magnus H. Sørby, Bjørn C. Hauback

Institute for Energy Technology, Physics Department, P.O. Box 40, NO-2027, Kjeller, Norway

ARTICLE INFO

Article history:
Received 15 August 2010
Received in revised form 5 October 2010
Accepted 15 October 2010
Available online 23 October 2010

Keywords:
Inorganic compounds
Powder diffraction
Fourier transform infrared spectroscopy (FTIR)
Differential scanning calorimetry (DSC)

ABSTRACT

Mechano-chemical routes to the metathesis reaction $4\text{LiBH}_4 + \text{VCl}_n \rightarrow \text{Li}_{4-n}\text{V(BH}_4)_4 + n\text{LiCl}$ ($n = 2$ and 3) are explored at room and liquid nitrogen temperatures. The produced samples consist of crystalline LiCl and unreacted LiBH_4. No other crystalline phases are observed directly by powder X-ray diffraction. The highest reactivity was observed when using VCl_3. Two possible reaction paths are proposed in order to explain this result: (a) $2\text{LiBH}_4 + \text{VCl}_2 \rightarrow 2\text{LiCl} + \text{VB}_2 + 4\text{H}_2$, with $\Delta H = -188$ kJ/mol and (b) $3\text{LiBH}_4 + \text{VCl}_3 \rightarrow 3\text{LiCl} + 1/2\text{B}_2\text{H}_6 + \text{VB}_2 + 9/2\text{H}_2$, with $\Delta H = -258$ kJ/mol. The calculated enthalpy values show that reactions with VCl_3 have stronger thermodynamical driving forces than with VCl_2, corroborating the experimental results. Still, the different experimental methods lead to the same final products, with longer milling times being necessary to remove the precursor traces in the case of VCl_2 and cryomilling. The results shed some light on the efficiency of mechano-chemical methods for the synthesis of mixed metal borohydrides based on LiBH_4 and V-chlorides.

1. Introduction

Despite its high stability, LiBH_4 is still amongst the most investigated hydrogen storage materials due to its high gravimetric capacity (18.4 wt.%). Many attempts are being carried out to accommodate its properties for practical applications. One of the most recent approaches involves the formation of new complexes, known as mixed metal borohydrides, from LiBH_4 and other alkali and alkaline-earth borohydrides [1,2]. As shown by Li et al. and Nakamori et al. [4,3], the stability of binary and mixed metal borohydrides correlates inversely with the Pauling electronegativity (χ_P) of the metal cation, and the averaged χ_P of the two metals, respectively. This allows the adjustment of the thermodynamical properties of the materials. First-principle calculations [4,5], and some successfull experimental cases (Li–Sc [6], Li–Zn [7] and Li–Mn [8]) have been reported.

In this work, the production of Li–V mixed metal borohydrides is attempted via mechano-chemical routes at room and liquid nitrogen temperatures. V has a $\chi_P = 1.63$, which is very close to that of Zn ($\chi_P = 1.63$). A mixed metal borohydride containing Li and V would have an average χ_P of 1.305, which lies in the proper enthalpy of formation range shown by the $248.7\chi_P - 390.8$ relation found by Li et al. [4]. The preparation of the samples is based on the metathesis reaction:

$$m\text{LiBH}_4 + \text{MCl}_n \rightarrow \text{Li}_{m-n}\text{M(BH}_4)_m + n\text{LiCl} \quad (1)$$

with M a transition metal. This type of reaction was first suggested by Jensen [9].

2. Experimental

Mixtures containing pre-milled LiBH4 (Aldrich, >95% purity) and commercial VCl_2 or VCl_3 (Sigma–Aldrich) in a 4:1 ratio, were mechano-chemically reacted in Ar using both planetary ball-milling (Fritsch Pulverisette 7), and cryomilling (Spex 6770 Freezer/Mill). The samples containing VCl_2 and VCl_3, respectively, are called Li–V_{II} and Li–V_{III} throughout the text. The experimental conditions are also specified in each case. A Gas pressure and Temperature Monitoring system vial (Fritsch GTM/II) was used in some cases to monitor the reactions during ball milling in a Fritsch Pulverisette 6 Mono Mill. The gas released during milling was analyzed with a MKS MicroVision Plus Residual Gas Analyzer (RGA). LiBH_4 was pre-milled in H_2 (20 bar) for 1 h using a Evico high-pressure vial. Sample handling was done in glove boxes filled with purified Argon (<1 ppm O_2, H_2O). Powder X-ray diffraction (PXD) patterns were collected using Cu Kα radiation in a Bruker AXS D8 Advance Diffractometer equipped with a Göbel mirror and a LynxEye™ 1D strip detector. The samples were packed and measured in rotating boron glass capillaries (0.5 and 0.8 mm Ø) filled and sealed under Ar atmosphere. Data acquisition was restricted to the $2\theta = 5$–80 range, with $\Delta 2\theta = 0.02$ and 2 s/step scanning rates. Differential Scanning Calorimetry (DSC) was carried out between room temperature (RT) and 600 °C in incoloy (high pressure—HP) crucibles or up to 500 °C in Al crucibles using a Setaram Sensys DSC. Temperature Programmed Desorption (TPD) was performed under dynamic vacuum up to 500 °C using an in-house built set-up. 2 °C/min heating rates were used for both DSC and TPD measurements. Raman (Jobin Yvon T64000) and Infrared (IR) (Bruker IFS 66v, with a DTGS detector) spectroscopies were performed only on selected samples. The powder was packed in capillaries for Raman and embedded in KBr pellets (7 and 10 mm Ø, with mass concentrations between 0.5 and 1%) for IR. The transmission (T) spectra were recorded in the 400–4000 cm^{-1} region, with a

---

* Corresponding author. Tel.: +47 63 80 62 09.
E-mail address: isabel.llamas@ife.no (I. Llamas-Jansa).

0925-8388/$ – see front matter © 2010 Elsevier B.V. All rights reserved.
doi:10.1016/j.jallcom.2010.10.070

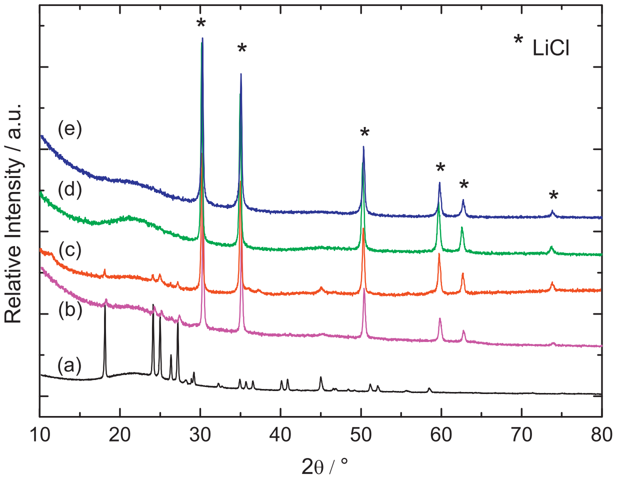

Fig. 1. PXD patterns for (a) pre-milled LiBH4; (b) ball-milled and (c) cryomilled Li–V_{II} samples; (d) ball-milled and (e) cryomilled Li–V_{III} samples. All the samples were measured after 1 h milling. Star symbols indicate the Bragg peak positions of the LiCl cubic phase. The remaining observed diffraction peaks belong to pure LiBH4.

1–5 cm^{-1} resolution, depending on the beam. Absolute mass absorption coefficients were calculated from the T data as:

$$\kappa = -\ln T\left(\frac{A}{m}\right) \tag{2}$$

where A is the area of the pellet in cm^2, and m is the sample mass in g [10].

3. Results and discussion

3.1. Structure and milling

While the PXD pattern from pre-milled $LiBH_4$ matches the reported orthorhombic structure of pure $LiBH_4$ at RT [11], the patterns obtained for the 1 h milled Li–V_{II} and Li–V_{III} samples are mainly characterized by crystalline LiCl, with lattice parameters between 5.137 and 5.144 Å (Fig. 1). In the case of Li–V_{II}, diffraction peaks corresponding to unreacted crystalline $LiBH_4$ are also observed between 15 and 30 for the samples milled for less than 2 h. No other crystalline phases are seen. Raman (not shown) and IR spectroscopy show the typical $BH4^-$-related features, with the stretching and deformation B–H modes in the 2150–2400 cm^{-1} and 1100–1300 cm^{-1} ranges, respectively (Fig. 2). Raman spectra are dominated by broad backgrounds, which are characteristic of high fluorescence signals induced by the dark coloured samples. This disguises inherently weak scattering signals [12]. IR vibrational data show more defined features, with the stretching band split into the three $2\nu_4$, ν_3, and $\nu_2+\nu_4$ contributions at 2385, 2293, and 2229 cm^{-1}, respectively. The bending mode is also split into a prominent ν_4 at 1125 cm^{-1} and a weak 1236 cm^{-1} band that becomes weaker in Li–V_{II} and Li–V_{III} with milling time. Bands at 1632, 1404 and 1002 cm^{-1}, known for pure $LiBH_4$ [13,14], are observed in the samples milled with VCl_2. These become weaker or disappear when using VCl_3. No evident shift of the vibration modes is observed. This indicates that the $BH_4{}^-$ force constant remains unchanged and no substitution of Li by V or $BH_4{}^-$ by Cl^- has occurred. This result differs from our findings on Na-transition metal samples (submitted), where the substitution of $BH_4{}^-$ groups by Cl^- anions is clearly indicated by the shifts of the infrared bands towards larger wavenumbers.

Differences between Li–V_{II} and Li–V_{III} are observed by PXD. In particular, $LiBH_4$ peaks are not present after 9 min milling in the Li–V_{III} case, while they can still be observed in Li–V_{II} after 1 and 2 h milling. This shows that although a 4:1 ratio was used for all the samples, the reaction proceeds further when using VCl_3. The effect is also observed indirectly by a significant increase of the pressure inside the vial during milling (Fig. 3). Note that the milling curve in the figure shows an experiment carried out for 3 h. The milling process was interrupted after 1 h and then let to rest. The bumps in the temperature and pressure curves are related to the sudden stop of the cooling system at the end of the milling. This causes an increase of temperature that affects the pressure at this particular point. The reaction is seen to proceed by an increase of the pressure until the amount of gas released reaches a 1.5 mol per mole of $LiBH_4$ (using the ideal gas law) plateau. Qualitative RGA of the gas released reveals the presence of both H_2 and B_2H_6 (Fig. 4) for this sample.

3.2. Thermal decomposition

DSC measurements (not shown) also show differences between the samples milled with VCl_2 and VCl_3. In the Li–V_{II} case, thwo major endothermic events are observed at approximately 100 and 300 °C. These correspond well with the orthorhombic-hexagonal phase transition and melting of $LiBH_4$. The peaks are slightly shifted compared to pure $LiBH_4$. The shift towards lower temperatures of the phase transition peak can be related to size reduction due to the mechano-chemical process. The shift towards higher temperatures of the melting and desorption peaks may be due to the

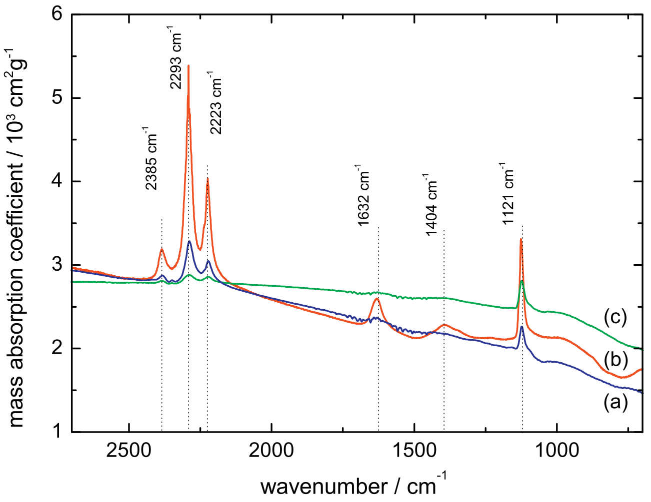

Fig. 2. IR absolute mass absorption coefficients for the 3 h cryomilled (a) Li–V_{III} and (b) Li–V_{II} samples; and (c) a 1 h ball-milled Li–V_{III} sample. Both the IR stretching and bending vibrational regions are shown and the major features indicated.

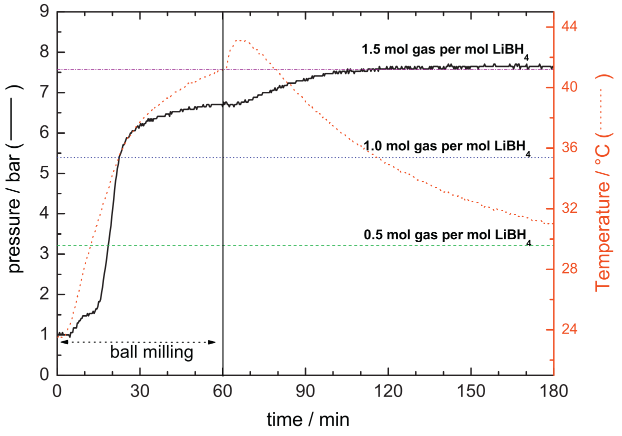

Fig. 3. Pressure (solid curve) and temperature (dashed curve) progression during (and after) ball-milling of a Li–V_{III} mixture. The major pressure steps after 10, 30, and 60 min can be observed in the first part of the curve. The milling process was interrupted after 1 h and then let to rest.

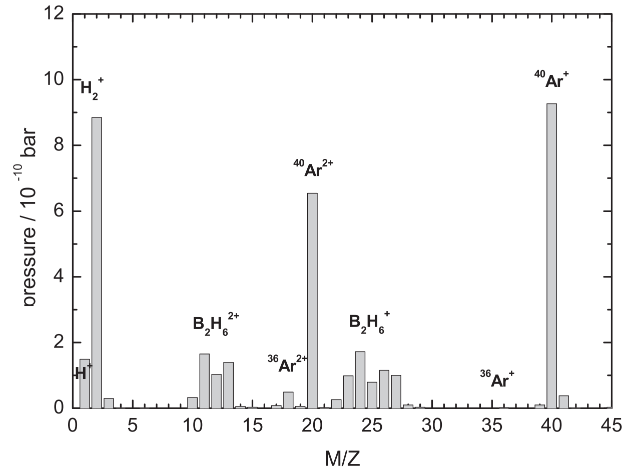

Fig. 4. RGA of the released gases inside the vial after 1 h ball-milling of a Li–V_{III} mixture.

presence of other species in the samples, such as Cl^- and/or V^- containing compounds in amorphous state. TPD curves reveal minor desorption events in the 100 °C range. Qualitative RGA suggests that this low-temperature desorption corresponds to a mixture of B_2H_6 and H_2. The main desorption occurs at 412 °C and is due to the unreacted $LiBH_4$. In contrast, DSC analysis of Li–V_{III} do not contain any heat-related event between 40 and 550 °C. This points out the almost complete reaction between $LiBH_4$ and VCl_3. The TPD curve of a cryomilled Li–V_{III} sample shows two desorption events, with maxima at about 125 and 225 °C, respectively. The latter feature occurs at too low temperatures to be related with the slight release of gas reported upon melting of pure $LiBH_4$ [11]. It might, however, indicate the presence of solid $B_{10}H_{14}$, which boils at 213 °C. Likewise, the desorption at 125 °C might indicate the presence of B_6H_{10}. This compund is liquid at room temperature and boils at 108 °C. However, there is no other indications of the formation of such compounds.

3.3. *Discussion: reaction pathways during mechano-chemical synthesis*

The results show that milling $4LiBH_4 + VCl_n$ mixtures leads mainly to the formation of crystalline LiCl. However, the detailed outcome of the mechano-chemical process depends on the milling conditions and the oxidation state of V. Unreacted $LiBH_4$ is seen by PXD and spectroscopy in all the samples, although the relative intensities of the IR mass absorption coefficient show a much smaller fraction when using VCl_3. This indicates that the reaction has proceeded in a larger extend for Li–V_{III} under the same conditions, which could be related to the reduction of V^{3+} into V^{2+} in a first step. The lack of a shift in the IR bands emphasizes that the $BH_4{}^-$ units are still part of $LiBH_4$ and not a substituted compound. No crystalline $LiBH_4$ is seen by PXD in Li–V_{III}, but the presence of solid B_xH_y-type boranes is suggested by TPD measurements. The amount of $LiBH_4$ that reacts with VCl_3 results in the formation of H_2 and B_2H_6. This is confirmed by RGA of a Li–V_{III} sample. Although the characterization methods used in this work do not provide direct information on V-containing phases it can be reasonably assumed to be in the form of amorphous $V_xB_x + 1$ compounds, since the formation of elemental V is unlikely under the experimental conditions [15]. Crystalline VB_2 is found at temperatures above 600 °C. Therefore, VB_2 might still be present in the $4LiBH_4 + VCl_n$ milled samples in an amorphous state. Based on the previous information, and considering that LiCl, VB_2, B_2H_6 and H_2 can be produced during ball milling of $4LiBH_4 + VCl_n$ mixtures, two tentative stoichiometric reactions, with a 2:1 and 3:1 ratio, respectively, are proposed:

$$2LiBH_4 + VCl_2 \rightarrow 2LiCl + VB_2 + 4H_2 \tag{3}$$

$$\Delta H = -188\,\text{kJ/mol};$$

$$3LiBH_4 + VCl_3 \rightarrow 3LiCl + \tfrac{1}{2}B_2H_6 + VB_2 + \tfrac{9}{2}H_2 \tag{4}$$

$$\Delta H = -258\,\text{kJ/mol}.$$

These two reactions are exothermic, with −188 and −258 kJ/mol for Li–V_{II} and Li–V_{III}, respectively [16]. The values show that Li–V_{III} reactions have stronger thermodynamical driving forces than Li–V_{II}, corroborating the experimental results. Moreover, in the case of Li–V_{III} (Eq. (4)), a 1.5 mol release of H_2 is expected, in agreement with the observed increase of pressure during milling. The excess of $LiBH_4$ observed experimentally is related to the original 4:1 ratio, which was chosen to fulfill Eq. (1).

A more detailed investigation on the effects of low/high milling temperatures is needed. This is particularly important for Li–V_{III} and the formation of high-molecular-weight boranes (B_xH_y).

4. Conclusions

The mechano-chemical process of $4LiBH_4 + VCl_n$ mixtures (with $n = 2$ and 3), leads to no mixed metal borohydrides under the applied experimental conditions. The products are composed of crystalline LiCl and excess $LiBH_4$, which is seen only in an amorphous state for Li–V_{III}. The different mechano-chemical methods lead to the same final product, although in some cases a longer milling time might be necessary to remove the precursor traces.

Acknowledgments

The NANOMAT and RENERGI programs of the Research Council of Norway are gratefully acknowledged for their finantial support. Prof. Claus Nielsen at the Chemistry Department of the University of Oslo is thankfully acknowledged for providing access to the Raman and IR spectrometers.

References

[1] E.A. Nickels, M.O. Jones, W.I.F. David, S.R. Johnson, R.L. Lowton, M. Sommariva, P.P. Edwards, Angewandte Chemie-International Edition 47 (2008) 2817–2819.
[2] R. Cerny, G. Severa, D.B. Ravnsbaek, Y. Filinchuk, V. D'Anna, H. Hagemann, D. Haase, C.M. Jensen, T.R. Jensen, Journal of Physical Chemistry C 114 (2010) 1357–1364.
[3] Y. Nakamori, H.-W. Li, K. Kikuchi, M. Aoki, K. Miwa, Journal of Alloys and Compounds 446–447 (2007) 296–300.
[4] H.W. Li, S. Orimo, Y. Nakamori, K. Miwa, N. Ohba, S. Towata, A. Züttel, Journal of Alloys and Compounds 446–447 (2007) 315–318.
[5] J.S. Hummelshøj, D.D. Landis, J. Voss, T. Jiang, A. Tekin, N. Bork, M. Dulak, J.J. Mortensen, L. Adamska, J. Andersin, J.D. Baran, G.D. Barmparis, F. Bell, A.L. Bezanilla, J. Bjork, M.E. Bjorketun, F. Bleken, F. Buchter, M. Burkle, P.D. Burton, B.B. Buus, A. Calborean, F. Calle-Vallejo, S. Casolo, B.D. Chandler, D.H. Chi, I. Czekaj, S. Datta, A. Datye, A. DeLaRiva, V. Despoja, S. Dobrin, M. Engelund, L. Ferrighi, P. Frondelius, Q. Fu, A. Fuentes, J. Furst, A. Garcia-Fuente, J. Gavnholt, R. Goeke, S. Gudmundsdottir, K.D. Hammond, H.A. Hansen, D. Hibbitts, E. Hobi Jr., J.G. Howalt, S.L. Hruby, A. Huth, L. Isaeva, J. Jelic, I.J.T. Jensen, K.A. Kacprzak, A. Kelkkanen, D. Kelsey, D.S. Kesanakurthi, J. Kleis, P.J. Klupfel, I. Konstantinov, R. Korytar, P. Koskinen, C. Krishna, E. Kunkes, A.H. Larsen, J.M.G. Lastra, H. Lin, O. Lopez-Acevedo, M. Mantega, J.I. Martinez, I.N. Mesa, D.J. Mowbray, J.S.G. Myrdal, Y. Natanzon, A. Nistor, T. Olsen, H. Park, L.S. Pedroza, V. Petzold, C. Plaisance, J.A. Rasmussen, H. Ren, M. Rizzi, A.S. Ronco, C. Rostgaard, S. Saadi, L.A. Salguero, E.J.G. Santos, A.L. Schoenhalz, J. Shen, M. Smedemand, O.J. Stausholm-Moller, M. Stibius, M. Strange, H.B. Su, B. Temel, A. Toftelund, V. Tripkovic, M. Vanin, V. Viswanathan, A. Vojvodic, S. Wang, J. Wellendorff, K.S. Thygesen, J. Rossmeisl, T. Bligaard, K.W. Jacobsen, J.K. Norskov, T. Vegge, Journal of Chemical Physics 131 (1) (2009).
[6] H. Hagemann, M. Longhini, J.W. Kaminski, T.A. Wesolowski, R. Cerny, N. Penin, M.H. Sørby, B.C. Hauback, G. Severa, C.M. Jensen, Journal of Physical Chemistry A 112 (33) (2008) 7551–7555.

[7] D. Ravnsbaek, Y. Filinchuk, Y. Cerenius, H.J. Jakobsen, F. Besenbacher, J. Skibsted, T.R. Jensen, Angewandte Chemie-International Edition 48 (36) (2009) 6659–6663.
[8] P. Choudhury, S.S. Srinivasan, V.R. Bhethanabotla, Y. Goswami, K. McGrath, E.K. Stefanakos, International Journal of Hydrogen Energy 34 (15) (2009) 6325–6334.
[9] G. Jensen, Tech. rep., U.S. DoE Hydrogen Program, Ann. Mer. Rev. Meet., 2007.
[10] I. Llamas-Jansa, Experimental study of the optical and structural properties of carbon nanoparticles, Phd Thesis, Friedrich-Schiller-Universität Jena, Jena, Germany, February 2006, ISBN: 3-8322-5063-8.
[11] A. Züttel, S. Rentsch, P. Fischer, P. Wenger, P. Sudan, P. Mauron, C. Emmenegger, Journal of Alloys and Compounds 356 (2003) 515–520.
[12] P. Matousek, M. Towrie, C. Ma, W. Kwok, D. Phillips, W. Toner, A. Parker, Journal of Raman Spectroscopy 32 (12) (2001) 983–988.
[13] H. Hagemann, Y. Filinchuk, D. Chernyshov, W. van Beek, Phase Transitions 82 (4) (2009) 344–355.
[14] E.R. Andresen, R. Gremaud, A. Borgschulte, A.J. Ramirez-Cuesta, A. Züttel, P. Hamm, Journal of Physical Chemistry A 113 (46) (2009) 12838–12846.
[15] L. Shi, Y. Gu, L. Chen, Z. Yang, J. Ma, Y. Qian, Materials Letters 58 (22–23) (2004) 2890–2892.
[16] A. Roine, Outokumpu HSC Chemistry for Windows, Version 5.1, 2002.